

Linkage and association of phospholipid transfer protein activity to *LASS4*^S

Elisabeth A. Rosenthal,* James Ronald,* Joseph Rothstein,* Ramakrishnan Rajagopalan,* Jane Ranchalis,* G. Wolfbauer,^{††} John J. Albers,^{**,*††} John D. Brunzell,^{§§} Arno G. Motulsky,^{*,†} Mark J. Rieder,[†] Deborah A. Nickerson,[†] Ellen M. Wijsman,^{*,†,§} and Gail P. Jarvik^{1,*†}

Division of Medical Genetics, Department of Medicine,* Department of Genome Sciences,[†] Department of Biostatistics,[§] Department of Pathology,^{**} Northwest Lipid Metabolism and Diabetes Research Laboratories, Department of Medicine,^{††} Division of Metabolism, Endocrinology, and Nutrition, Department of Medicine,^{§§} University of Washington, Seattle, WA

Abstract Phospholipid transfer protein activity (PLTPa) is associated with insulin levels and has been implicated in atherosclerotic disease in both mice and humans. Variation at the *PLTP* structural locus on chromosome 20 explains some, but not all, heritable variation in PLTPa. In order to detect quantitative trait loci (QTLs) elsewhere in the genome that affect PLTPa, we performed both oligogenic and single QTL linkage analysis on four large families (n = 227 with phenotype, n = 330 with genotype, n = 462 total), ascertained for familial combined hyperlipidemia. We detected evidence of linkage between PLTPa and chromosome 19p (lod = 3.2) for a single family and chromosome 2q (lod = 2.8) for all families. Inclusion of additional marker and exome sequence data in the analysis refined the linkage signal on chromosome 19 and implicated coding variation in *LASS4*, a gene regulated by leptin that is involved in ceramide synthesis. Association between PLTPa and *LASS4* variation was replicated in the other three families ($P = 0.02$), adjusting for pedigree structure. **To our knowledge, this is the first example for which exome data was used in families to identify a complex QTL that is not the structural locus.**—Rosenthal, E. A., J. Ronald, J. Rothstein, R. Rajagopalan, J. Ranchalis, G. Wolfbauer, J. J. Albers, J. D. Brunzell, A. G. Motulsky, M. J. Rieder, D. A. Nickerson, E. M. Wijsman, and G. P. Jarvik. **Linkage and association of phospholipid transfer protein activity to *LASS4*.** *J. Lipid Res.* 2011. 52: 1837–1846.

Supplementary key words cardiovascular disease • exome analysis • linkage analysis • complex trait

Cardiovascular disease (CVD) is a leading cause of death in the United States. Lipid transfer proteins play a major

This work was supported by the National Institutes of Health grants R01 HL67406, P01 HL030086, T32 GM007454, R01 HL094976, R37 GM046255, and RC2 HG005608 with additional support from the Northwest Institute of Genetic Medicine and the State of Washington Life Sciences Discovery Fund. Its contents are solely the responsibility of the authors and do not necessarily represent the official views of the National Institutes of Health or other granting agencies.

Manuscript received 20 April 2011 and in revised form 8 July 2011.

Published, JLR Papers in Press, July 13, 2011
DOI 10.1194/jlr.P016576

Copyright © 2011 by the American Society for Biochemistry and Molecular Biology, Inc.

This article is available online at <http://www.jlr.org>

role in the regulation of lipids and therefore may be involved in CVD (1–4). Phospholipid transfer protein (PLTP) is physically associated with HDL, produced in the liver and other tissues, and involved in the transfer of cholesterol and phospholipids from VLDL to HDL (1, 5, 6) and remodeling of HDL (7). PLTP is also expressed in macrophages and may modulate their transformation into foam cells (8, 9). Improved understanding of the regulation of *PLTP* and its activities may result in better prevention, management, and treatment of CVD.

Studies in mice provide evidence of a role of *PLTP* in lipoprotein levels and atherosclerosis. Overexpression of *PLTP* in mice results in an increase of pre β -HDL (10–13), a decrease in HDL (11), reduced LDL and VLDL levels (14), and atherosclerosis (12, 14–18). Elevation of plasma *PLTP*, rather than macrophage *PLTP*, impaired reverse cholesterol transport in transgenic mice (16). Human *APOB* transgenic mice that were deficient in *PLTP* had reduced levels of apoB containing lipoproteins and reduced atherosclerosis (19). Inhibition of *PLTP* activity (PLTPa) also lowered apoB levels (20). PLTPa is highly positively correlated with HDL size and concentration among inbred mouse strains (21).

In human studies, both *PLTP* mass and PLTPa, which are weakly correlated (22), have been shown to be associated

Abbreviations: adj-PLTPa, residuals from adjusted phospholipid transfer protein activity model; BF, Bayes factor; BMI, body mass index; chr., chromosome; CVD, cardiovascular disease; FCHL, familial combined hyperlipidemia; GERP, Genomic Evolutionary Rate Profiling score; hsCRP, C-reactive protein level; IBD, identical by descent; LD, linkage disequilibrium; ln, natural log; lod, logarithm of odds; MCMC, Markov chain Monte Carlo; *PLTP*, phospholipid transfer protein; PLTPa, PLTP activity; QTL, quantitative trait locus; SNP, single nucleotide polymorphism; STR, Single Tandem Repeat; TG, triglyceride; var(adj-PLTPa), variation in adj-PLTPa.

¹To whom correspondence should be addressed.

email: gjarvik@medicine.washington.edu

^SThe online version of this article (available at <http://www.jlr.org>) contains supplementary data in the form of three figures, one table, and supplementary methods.

with lipid traits, glucose regulation, and atherosclerosis. PLTP mass is associated with HDL size and concentration (22, 23) whereas PLTPa is associated with total cholesterol, VLDL and LDL cholesterol, and apoB level (22, 24, 25). PLTPa is positively correlated with insulin and glycosylated hemoglobin (HbA1C) (26) and decreases in response to insulin infusion (27, 28).

To date, only structural-locus genetic variation is known to influence PLTPa in humans. In humans, common variation at the *PLTP* structural locus region has been shown to explain $\leq 30\%$ of variation in PLTPa (26). *PLTP* variants were found to be associated with PLTP mRNA level (29) and with cardiovascular disease risk (23, 26).

Given that multiple genes influence PLTPa in mice (30), we investigated the hypothesis that quantitative trait loci (QTLs) in regions of the genome other than the *PLTP* structural locus affect PLTPa in humans. Such QTLs might also impact atherosclerotic risk as well as shed light on the mechanisms regulating PLTPa. We have previously shown that regulatory region variants at *PLTP* influence PLTPa in the four large families investigated here (26). This family-based design allows the detection of QTLs within single large families, which accommodates potential locus heterogeneity among families.

METHODS

Subjects

The sample includes four large families of European-American descent who were ascertained in the 1980s for familial combined hyperlipidemia (FCHL) and large sibships (31). From 2003 to 2008, recollection of 234 family members expanded pedigree structures and provided samples for PLTPa measurement (26, 32). Although the families were ascertained for FCHL, PLTPa in these families does not differ from that in the European-American population as a whole (26). **Table 1** displays the sample size characteristics of the family data. There are four families, labeled F1, F2, F3, and F4, consisting of 462 individuals, 227 of whom have measured PLTPa and 330 of whom have genetic data. All study participants or their representatives gave written informed consent. The University of Washington Human Subject Review Board (FWA #00006878) approved this study.

Phenotypes

In addition to descriptive (sex, age, height, weight) covariates, we measured cardiovascular risk phenotypes. These covariates included LDL, HDL, apoA1, apoB, total cholesterol, triglycerides (TGs), glucose, insulin, and C-reactive protein (hsCRP) level.

TABLE 1. Total number of individuals with phenotype data, by family

Family	Num (M/F)	Age mean (range)	PLTPa (M/F)
F1	142 (70/72)	50 (13,89)	82 (37/45)
F2	94 (51/43)	43 (11,85)	55 (25/30)
F3	121 (67/54)	47 (15, 71)	41 (21/20)
F4	105 (55/50)	47 (20,87)	49 (24/25)
all	462 (243/219)	47 (11,89)	227 (108/119)

All individuals are European-American. The second column from the left indicates the total number of individuals (males/females). The column on the right indicates the number of individuals with measured PLTPa (males/females).

Insulin, glucose, hsCRP, and TG were natural log (ln) transformed. Body mass index (BMI) was calculated for all individuals with both height and weight data and imputed for 17 of 227 individuals using linear regression on age, sex, age by sex, and ln(hsCRP) (33). Insulin was not collected on 20 individuals from family F3 who were collected prior to a change in protocol. Therefore, ln(insulin) was imputed for these individuals using linear regression on sex, age, ln(TG), and BMI.

Covariate selection, using a linear model, was used to adjust PLTPa. Residuals from this model (adj-PLTPa) were subsequently used for all analyses. Although the significance of each covariate may be affected by the underlying structure imposed by the relationships in the families, the mean estimated effects are not biased (34). Thus, covariate adjustments do not need to be conditioned on family structure.

Laboratory measures

PLTPa was measured in vitro as described elsewhere (26, 35). Briefly, PLTP-mediated transfer of plasma phospholipids was calculated on fasting whole plasma by measuring the percent transfer of ^{14}C -phosphatidylcholine from phospholipid liposomes to HDL. PLTPa and lipids were measured at the Northwest Lipid Metabolism and Diabetes Research Laboratories, blinded to all other subject data. Measurements were performed on fasting whole plasma as detailed elsewhere (36). Insulin was measured by double antibody radioimmunoassay. Each assay included appropriate reference samples.

Genotyping

Genotypes, using several platforms, were measured on the families.

STR markers. Marshfield panel 9 Single Tandem Repeat (STR) markers were collected on the originally ascertained family members. Dense marker genotyping was also performed for selected regions at DeCode Genetics (32). Individuals ascertained since 2002 and 8 from the original ascertainment were typed on the Prevention Genetics marker set 13, which overlaps Marshfield panel 9. Data cleaning and quality control analyses on the marker genotypes were carried out as described elsewhere (32, 37). Prevention Genetics genotype information was removed for five individuals because their genotype data had high homozygosity ($>15\%$), indicating poor amplification of their DNA. In seven instances where individual marker genotype transmission errors were detected in the Prevention Genetics data, the genotypes from the Marshfield panel did not cause a transmission error; therefore, the Marshfield genotypes were used in these cases. In all other cases, genotypes for the direct descendants, siblings, and parents of an individual involved in a marker transmission error were removed. After data cleaning, genotypes were available for 330 subjects, averaging 470 marker genotypes per individual (min = 180, max = 658). Average distance between markers was 5.4 cM (SD = 4.1).

SNP markers. The families were also genotyped using the Illumina HumanCVD Bead chip (38). The Illumina chip contains $\sim 50\text{K}$ single nucleotide polymorphisms (SNPs) in and near genes of interest to CVD. SNPs from this chip were selected for inclusion in this analysis based on linkage disequilibrium (LD) ($r^2 \leq 0.8$) in a second cohort of unrelated European Americans ($n = 924$), described in detail elsewhere (26, 39). All markers and SNPs were aligned to the Rutgers build35 marker map (40). All analyses were based on assumption of a Haldane map function (41) with map locations interpolated for markers and SNPs that had only a physical map location (see supplementary material).

Exome markers. Exome target region capture and sequencing on the Solexa platform was performed as previously described (42) in anticipation of multiple linkage peaks. This design is more efficient than sequencing specific regions of the genome when multiple traits or multiple families are under analysis. Exome sequencing was performed on 54 individuals from the four families who were selected for extreme PLTPa or other CVD-related phenotypes and the presence of close relatives with genotype data. We used the Genome Analysis Toolkit Unified Genotyper (43) to derive sequence calls from the raw reads. Low confidence sites were defined by at least one of the following: quality score <50 , allelic balance >0.75 , variant allele homopolymer run >3 , or the variant confidence divided by the quality by depth <5 , and were excluded from analysis. Selected exomic variants were followed up by genotyping of all pedigree members with available DNA using standard PCR methods. In each case, the exomic variants genotypes were confirmed and the variants segregated in a Mendelian fashion. Exome genotyping quality control, including comparison of identity by descent regions, is discussed in the supplementary material.

Linkage analysis

The analysis strategy for adj-PLTPa was 1) oligogenic QTL linkage analysis to identify regions of interest and propose trait models, 2) fixed-model single QTL linkage analysis to compute lod scores in the regions of interest, 3) determination of the region containing the shared segregating haplotype, and 4) incorporation of single-site CVD chip or exomic genotypes in the region of interest to determine which genes, if any, contribute to the linkage signal. Each of these steps involves use of methods that employ the sampling-based approach of Markov chain Monte Carlo (MCMC). This allows for efficient analysis of complex traits on large pedigrees with full use of multipoint marker data and inclusion of multilocus trait models. Further, these complementary analysis methods maximized the strengths of each method to detect linkage and refine the signal. Because incorporating multiple SNPs in the oligogenic analysis is inefficient given availability of highly-informative STR markers, this approach also minimizes computational time. Run conditions for the MCMC-based methods are given in the supplementary material.

Because PLTPa is a complex trait whose segregation has not previously been studied, no proposed genetic models existed. Therefore, initial analysis used the oligogenic QTL method implemented in the Loki package, ver. 2.4.7 (44). This approach has several advantages. First, the parameters for a trait model are not specified. Instead, only prior distributions for the number of QTLs and their possible effects are specified. Second, similar to a variance components approach, covariates can be included in the model and their effects estimated. Also, the parameters for a trait model are not specified. Third, unlike a variance components approach, a QTL model can be inferred from the jointly estimated posterior distributions for the location, allele frequency, and genotype effects of putative QTLs. Also, the proportion of genetic variation due to each QTL is output for each iteration as well as the residual and genetic variances, from which heritability can be estimated. We estimated heritability of adj-PLTPa in each family as the average heritability over all saved iterations. One drawback to this method is that calculating p-values is time consuming as it requires determining an empirical distribution (45). However, because the analysis is Bayesian (i.e., based on estimated posterior distributions given the data and prior distributions), we chose locations for further analysis based on the Bayes factor (BF), which compares the posterior and prior odds of a QTL

in a region (45–48). The larger the BF, the more evidence there is for the posterior distribution. We followed up regions with a maximum BF (maxBF) ≥ 25 , calculated over 2 cM intervals. We consider a BF < 0.32 ($\log(\text{BF}) < -0.5$) as evidence against linkage.

We followed up the regions of interest, using multipoint logarithm of odds (lod) score linkage analysis. Computations were carried out with the program `lm_markers` from the Morgan package (49–51), which is, to the best of our knowledge, the only program capable of carrying out a model-based multipoint analysis for a quantitative trait on large pedigrees. This analysis method requires a prespecified single locus trait model and provides a lod score and p-value. Such fixed-model analyses are very powerful if the trait model is correctly specified (52, 53) and are unlikely to produce false-positive evidence for linkage when the trait model is misspecified (54–57), especially in larger pedigrees (52). Estimation of the QTL model parameters is discussed in the supplementary material.

Refining regions of interest

In order to narrow genomic regions where $\text{lod} > 3$, we searched for a haplotype segregating with adj-PLTPa among influential individuals. An individual was considered influential if removal of their phenotype reduces the lod score to <3.0 . We calculated the probability that an allele is shared identical by descent (IBD) among the influential individuals using results from the program `gl_auto` from the Morgan package (58). We considered an ancestral haplotype to be shared IBD among groups of individuals if the IBD probability for the ancestral allele at each marker on this haplotype was ≥ 0.75 . We used both STR marker and CVD SNP data in order to determine the most likely boundaries for the haplotype.

Follow-up using CVD SNP chip and exome sequence data

For regions with consistent supportive evidence for linkage, we further evaluated the effect of variant sites in a measured genotype approach (59). We used both SNP and exomic sequence data and determined the proportion of the total variation in adj-PLTPa [$\text{var}(\text{adj-PLTPa})$], explained by each variant as a covariate, using the analysis method in Loki. For these follow-up analyses, 5×10^4 MCMC iterations were used. An advantage of using Loki for this analysis is that missing genotypes are imputed using the segregation information and genotypes of other family members, so that all individuals with phenotype information are included in the analysis (32). In the cases where the hapmap CEU (European-American) allele frequency (q) was unknown, we used $q = 0.01$. Sites that explain a large portion of the $\text{var}(\text{adj-PLTPa})$ are expected to be in strong LD with the causal variant (60). Because SNPs were available for many more individuals than exomes, the estimated effects from the exome analysis have higher variance and lower power to account for a linkage signal. Additionally, an upward bias for effect size is expected in the exome analysis because individuals chosen for exome sequencing had extreme adj-PLTPa (61). Therefore, we genotyped sites of interest in the remaining family members and verified the linkage and association with adj-PLTPa. In addition, we estimated the percent genetic $\text{var}(\text{adj-PLTPa})$ explained in the families. Association with adj-PLTPa was also verified using variance components analysis from the SOLAR package (62), which adjusts for pedigree structure and provides an unbiased p-value for the association. Although we evaluated all exomic sites within the region, we emphasized those sites within genes expressed in the tissues most relevant to plasma PLTPa (liver, adipose, vascular epithelium, or intestine).

RESULTS

Covariate selection and outliers

The previously identified covariate model for adj-PLTPa included age, sex, age by sex interaction, BMI, and $\ln(\text{insulin})$, explaining 16% of the total var(PLTPa) in the families (26). The distribution of adj-PLTPa residuals in the families are shown in **Fig. 1**. The residuals are essentially normally distributed with mean zero and variance 5.24 for all families. The mean adj-PLTPa of individual families was not significantly different from the mean of all families except for family F3 ($P = 0.03$). The higher adj-PLTPa in F3 is not explained by outliers. Although there are a few outliers from other families, removing or Winsorizing (63, 64) their phenotypes did not impact the results of the linkage analyses. Heritability was estimated at 0.55, 0.25, 0.38, and 0.24 for families F1, F2, F3, and F4, respectively, and 0.42 over all families. *PLTP* structural locus SNP rs6065904, which has been shown to be associated with PLTPa and mRNA level (23, 26), explained 5% of the genetic var(adj-PLTPa) in the families; adjustment for this SNP did not impact linkage results, as noted below.

Oligogenic PLTPa QTL linkage results

We identified evidence of linkage to three chromosomes (chrs.). **Figure 2** displays the BF across the genome for all families and each individual family. Joint analysis of all families supports linkage to chrs. 1 and 2 (Fig. 2all, maxBF = 67 and 41, respectively). Individually, none of these families shows strong support for either chr. 1 or 2. Analysis on F1, the largest family, supported linkage to chr. 19 (Fig. 2F1, maxBF = 54). Because these results support genetic heterogeneity, further analyses considered F1 only for linkage to chr. 19 and all families for linkage to chrs. 1 and 2. Notably, we did not detect evidence for linkage to the structural locus on chr. 20, even when including SNPs near *PLTP*, nor did we find any coding variation in the *PLTP* exons in the sequenced individuals. Known functional 5' *PLTP* SNPs, when included as a genotype covariate, did not substantially change the linkage results (not shown).

Regional QTL analysis

Fixed-model lod score linkage analysis resulted in further evidence for linkage to chr. 19, supported linkage to chr. 2, and decreased support for chr. 1 (**Table 2**). Model estimates are provided in the supplementary data. On chr. 19, the maximum lod score, lodmax = 3.2, occurred at D19S1165 (33.43 cM). On chr. 2, lodmax = 2.8, at D2S434 (222.24 cM). On chr. 1, lodmax = 1.6 near D1S2141 (230.42 cM). Because the overdominant models estimated for QTLs on chrs. 1 and 2 are biologically unlikely, a dominant model was obtained for these two chrs. by fixing the heterozygote effect equal to the minor homozygote effect. Use of the estimated overdominant versus dominant models did not markedly change the linkage evidence for either chr. 1 or 2. Because only chr. 19 had a lod score > 3, we chose to pursue this signal with the CVD and exome SNPs.

Refining region of interest on chr. 19

A haplotype on chr. 19 was found to segregate with adj-PLTPa, further narrowing the region of interest. The haplotype spans the region between rs12608849 and D19S1165 (25.05–33.43 cM) (**Table 3**). Six individuals from family F1 were influential to the lod score in that removal of their phenotype lowered the lod score from 3.2 to between 2.75 and 2.89. Of the six influential individuals, four had adj-PLTPa values in the upper quartile of the distribution and carry this haplotype IBD with joint probability ≥ 0.8 at any individual marker on the haplotype. The other two influential individuals do not carry this haplotype and had adj-PLTPa values in the lower quartile as expected. Notably, the LDL receptor gene, *LDLR*, lies within the IBD region (~ 32 cM).

Chromosome 19 QTL follow-up using CVD SNP chip and exome sequence data

We investigated the region between 19 and 37 cM (6 Mb – 14.5 Mb), which includes the region with the shared haplotype segregating with adj-PLTPa. By including a larger region that contains the shared haplotype, we conservatively allowed

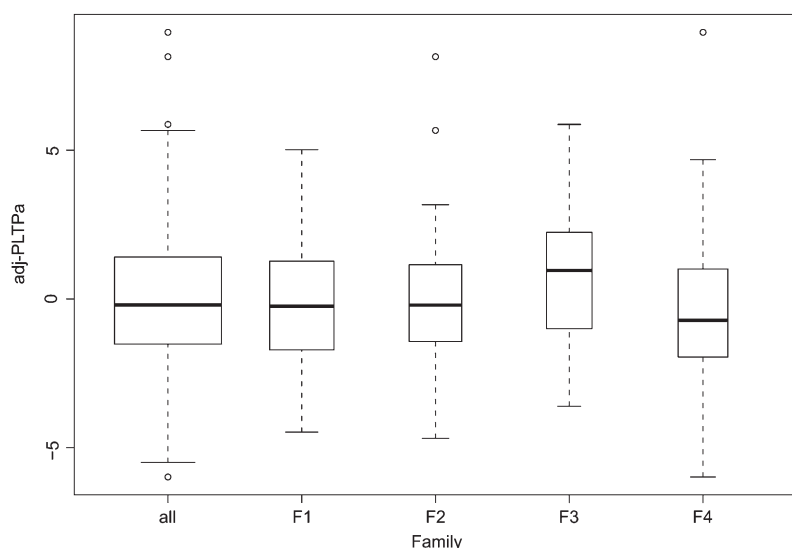


Fig. 1. Distribution of adj-PLTPa for all families and each individual family (F1–F4). The width of each boxplot is proportional to the number of individuals with measured PLTPa (Table 1). For all boxplots, the box encloses the interquartile range, the thick line represents the median, and the whiskers extend to the data point that is closest to and less than 1.5 times the interquartile range. Circles beyond the whiskers are more extreme points.

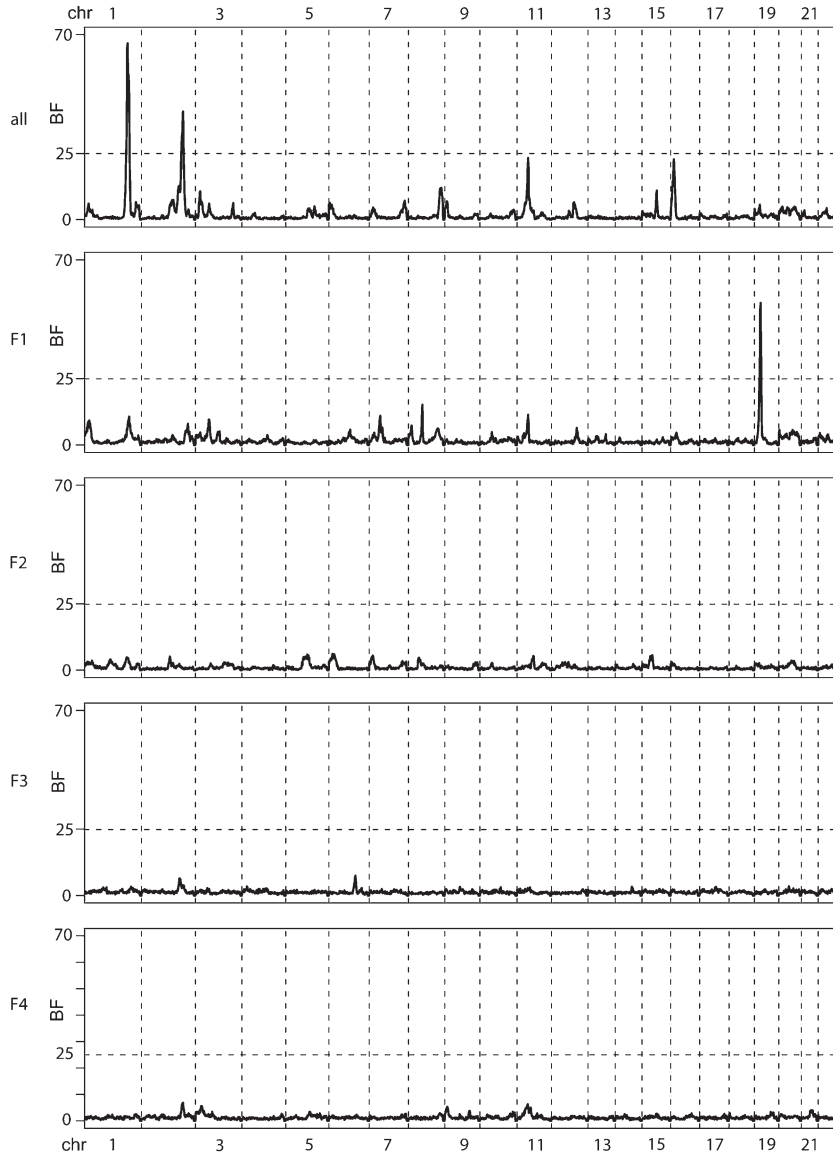


Fig. 2. Bayes factor versus chromosomal location for adj-PLTPa linkage. Shown are all families and individual families F1–F4. The dotted line at 25 represents the cutoff used to select regions for further analysis.

for the possibility that a variant outside of the IBD region influences adj-PLTPa. In this larger region, CVD SNPs rs10418380 and rs12463361 explained 15% and 13% of the total $\text{var}(\text{adj-PLTPa})$, respectively. The exome data included 496 variant sites spanning 143 genes: one nonsense,

TABLE 2. Trait models used in, and results from, model based linkage analysis

Chr.	p_1	γ_{11}	γ_{12}	γ_{22}	V_e	Lodmax
19	0.76	0	2.8	3.6	1.7	3.2
2	0.92	0	3.7	3.7	3.5	2.8
1	0.91	0	3.9	3.9	3.1	1.6

The trait models were estimated from the oligogenic analysis in Loki and consist of the allele frequency of the reference allele (p_1), the heterozygote effect, γ_{12} , and the alternative homozygote effect, γ_{22} . The models are set so that $\gamma_{22} \geq \gamma_{11}$. Because the estimated model on chrs. 2 and 1 were overdominant, we set $\gamma_{22} \equiv \gamma_{12}$. The within genotype environmental variance (V_e) is the difference between the total variance of adj-PLTPa and the genetic variance.

222 missense, 234 coding synonymous, 30 intronic, and nine in the noncoding region. Of these, there were 308 variants in 96 genes expressed in either liver, adipose, vasculature, or intestine, our tissues of interest. There was a true gap in coding genes within a 4 cM region of the IBD segment (**Fig. 3**, supplementary Fig. II). This region has low recombination and contains mostly olfactory receptor genes, which are unlikely to impact PLTPa (supplementary Fig. III). Exome coverage and missing data rates in this region did not differ from the rest of chr. 19 (data not shown).

Analysis of the exomic variants both within the IBD region and in genes expressed in tissues of interest identified four nonsynonymous candidate sites (**Table 4**, Fig. 3) that explained >12% of total $\text{var}(\text{adj-PLTPa})$. Two of these sites, rs17160348 and rs17160349, are missense variants in the longevity assurance homolog 4 gene, *LASS4*, each explaining 13% of the total $\text{var}(\text{adj-PLTPa})$. These variants

TABLE 3. Joint probability of sharing the ancestral allele among influential individuals in F1

Marker	Location (cM)	UQ	All
D19S1034	19.28	0.05	0.05
rs2860177	24.15	0.69	0.63
rs12608849	25.05	0.8	0.74
D19S586	30.04	0.95	0.93
D19S581	32.35	0.96	0.96
rs5742911	32.4	0.96	0.96
D19S1165	33.43	0.96	0.96
rs9917042	35.4	0.63	0.63
rs12463361	37.7	0.27	0.27
D19S714	39.54	0.001	0.001

Column UQ, probability that the four influential individuals with adj-PLTPa values in the upper quartile share the allele IBD. Column All, probability that the two influential individuals with values in the lower quartile of the distribution do not share this allele IBD with the other four influential individuals. Probabilities > 0.75 are in bold.

each have minor allele frequency of 0.16 in Caucasians, and the positions are evolutionarily conserved with Genomic Evolutionary Rate Profiling score, (GERP) = 2.99 and 2.89, respectively (65). Another missense variant in *LASS4*, rs36259, with minor allele frequency of 0.22, was successfully called on 16 of the 26 family members and explains 11% of the total var(adj-PLTPa). Although rs17160348 and rs17160349 are in complete LD in the 1000 genomes CEU sample (66), one subject's exome sequence was discordant. After directly genotyping these two sites in all families, it was apparent that a calling error existed in the exome data and that the sites were in complete LD in all four families as expected for European-Americans. We did not genotype rs36259 because the

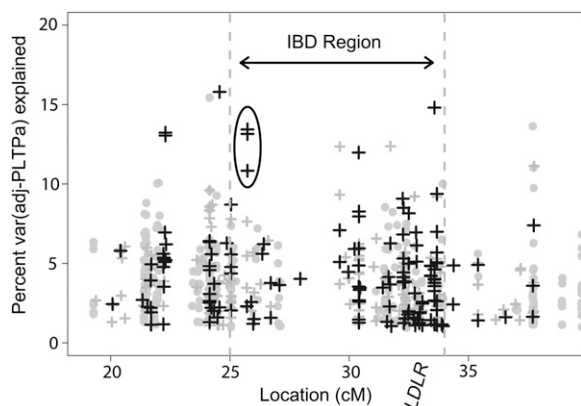


Fig. 3. Total variance of adj-PLTPa explained in family F1 by sites in chr. 19 regional genes expressed in at least one of the following tissues: liver, intestine, adipose, or vascular epithelium. Black crosses are nonsynonymous variants. Gray crosses are synonymous variants. Gray dots are CVD SNPs. The IBD region from Table 3 is indicated. The *LASS4* variants are circled. The differences in exome results among the three concordant *LASS4* variants are due to an exome calling error at rs17160349 and only 16 of 26 exomes called at rs36259. Upon full genotyping, the *LASS4* variant rs17160348 was significantly associated with adj-PLTPa in families F2, F3, and F4 ($P = 0.02$). The site in *OLFM2*, located at 30.4 cM, was not significantly associated with adj-PLTPa in families F2, F3, and F4 ($P = 0.75$), nor was the site in *ZNF443*, located at 33.6 cM ($P = 0.71$). The location of the LDL receptor gene (*LDLR*) is indicated.

minor alleles of the other two sites always occur with the minor allele of rs36259 in the 1000 genomes CEU sample ($D' = 1$, $r^2 = 0.7$) (66), as well as with the inherited haplotype in our data. Because these three sites had identical genotypic states in family F1, they identified a haplotype shared by family members (Table 5, haplotype B), and results for each site were identical. Including all available genotypes at rs17160348 explained 6% of total var(adj-PLTPa) and 19% of genetic var(adj-PLTPa) in family F1, and reduced the maxBF to 18 from 54. The minor allele appeared to increase PLTPa in family F1 (Fig. 4A). Two siblings in family F1 had a separate predicted deleterious missense mutation at rs17159388, inherited from a founder outside the pedigree. Additional alleles such as this are not accommodated in the linkage model and may result in rs17160348 not explaining all of the linkage evidence.

In addition to the single discovery family, the rs17160348 genotype association with adj-PLTPa was validated in the three other families ($P = 0.02$). Because there were only two minor homozygotes, we estimated the dominance effect coefficient $\beta_{\text{dom}} = 1.2$, which was in the same direction as the effect in family F1 (Fig. 4). Measured across these three families, the *LASS4* variant explained 20% of the genetic var(adj-PLTPa). However, the *LASS4* variant was not associated with HDL, LDL, VLDL, TG, apoB, total cholesterol, or insulin ($P > 0.26$) in any of the families.

Unlike the *LASS4* variants, the association at the other two nonsynonymous SNPs in the haplotype was not replicated in the other three families ($P = 0.71$ for rs28559848 and $P = 0.75$ for rs11556087). These SNPs occur in the zinc finger protein 443 gene, *ZNF443*, and in the Olfactomedin 2 gene, *OLFM2*, a gene relevant to glaucoma (67). The minor allele of rs28559848 causes a read through at *ZNF443*, resulting in four extra amino acids, and the site is not evolutionarily conserved (GERP = -2.71). This site's genotypes cluster poorly, possibly due to interference of nearby zinc finger genes, leading to missing data and decreased confidence in genotype calls. SNP rs11556087 results in a missense in *OLFM2* and is evolutionarily conserved (GERP = 3.6). Other variants on the risk haplotype, but not expressed in relevant tissues, are discussed in the supplementary material. Only synonymous coding variants were detected at *LDLR*, none of which explained the var(adj-PLTPa).

DISCUSSION

We presented evidence of linkage between PLTPa and chrs. 19 and 2. The linkage evidence on chr. 19 was attributable to a single family (F1), whereas detection of linkage on chr. 2 required information from all four families. Among biologically plausible genes on the linked inherited haplotype (IBD region) on chr. 19, only *LASS4* contained variants that were significantly associated with PLTPa in both the discovery family and the three additional families; these effects are also in the same direction. Failure to detect linkage between chr. 19 and families F2, F3, and F4 does not negate the observed association. Including *LASS4* haplotype from all available F1 pedigree

TABLE 4. Genes for which variant exomic sites explain $\geq 12\%$ of the total var(adj-PLTPa)

Gene	rsID	Loc. (cM)	IBD	maf	V	GERP	Effect
EMR1	rs373533	22.3	Unlikely	0.22	0.13	-0.72	missense
EMR1	rs461645	22.3	Unlikely	0.23	0.13	-0.24	missense
FCER2	rs2228137	24.6	Unlikely	0.03	0.16	2.83	missense
FBN3	rs12460643	25.1	Possibly	0.29	0.22	-7.7	synonymous
FBN3	rs12974280	25.2	Possibly	0.37	0.13	-5.17	synonymous
LASS4	rs17160348	25.7	Yes	0.16	0.13	2.99	missense
LASS4	rs17160349	25.7	Yes	0.16	0.13	2.89	missense
ZNF317	rs9305035	29.6	Yes	0.08	0.13	2.57	synonymous
OLFM2	rs11556087	30.4	Yes	0.24	0.12	3.6	missense
TYK2	rs280523	31.7	Yes	0.10	0.13	-3.42	synonymous
ZNF625	rs12972621	33.4	Yes	0.42	0.13	1.27	synonymous
ZNF443	rs28559848	33.6	Likely	0.19	0.12	-2.71	nonsense
DNAJB1	rs3962158	37.8	Unlikely	0.32	0.12	-6.54	Synonymous

A positive GERP score indicates evolutionary conservation of the reference allele (65). Genes in bold type are expressed in at least one of four relevant tissues: liver, intestine, adipose, or vascular epithelium. The column labeled IBD indicates if the site is within the IBD region. V, var(adj-PLTPa) explained; maf, minor allele frequency in hapmap CEU.

members explained some, but not all, of the chr.19 linkage evidence for PLTPa. This suggests that other regional variation, such as alternative alleles, may contribute to variation in PLTPa or that the linear model construct is insufficient to model the underlying biology.

The *LASS4* haplotype associated with PLTPa carried three separate missense mutations in all families. Phenotypic effects could be due to one or all of these. The rs17160348 variant causes a Ala353Val amino acid (aa) substitution (of 394 aa) and is highly conserved (GERP = 3.0). Further, this A/V is likely to disrupt an α helix and rs17160348 is a cis-eQTL modifying *LASS4* liver expression (68). As the minor allele for rs17160349 (Arg379Gln) is always paired with that of rs17160348, they have similar GERP scores (~ 3). rs36259 (Ala366Thr) is only slightly less conserved (GERP = 1.7).

LASS4 is an interesting and plausible biological candidate for influencing PLTPa. *LASS4* is involved in sphingolipid synthesis, specifically of longer ceramides (69). Adipose ceramide correlates with fatty liver and inflammation (70). *LASS4* is expressed in most tissues, including adipose and liver, although not in muscle, testis, or thymus (71, 72). Noncoding genetic variation in *LASS4* is associated with variation in sphingomyelin species C18 to C20, with ceramide C20:0, and ratios of sphingolipids (73). In rodent models, leptin infusion downregulates *LASS4* and decreases ceramide production in adipose; this decreased ceramide is associated with decreased insulin resistance (74). As discussed above, PLTPa is correlated with insulin and HbA1C levels and is altered by insulin or glucose infusion (26–28). An association between insulin and rs17160348 is not expected as PLTPa was adjusted for insulin in our analysis. Furthermore, adj-PLTPa was only weakly correlated with HDL, LDL, VLDL, TG, apoB, and total

cholesterol consistent with the lack of association found between the *LASS4* variants and these phenotypes. To our knowledge, *LASS4* variants have not been reported to be associated with these traits or cardiovascular disease.

Inability to detect a linkage signal at the *PLTP* structural locus on chr. 20 may have been due to the absence of large-impact rare variants at the locus in these families, or the presence of multiple alleles with smaller impacts on PLTPa. Consistent with this, no *PLTP* coding variants were detected by exome sequencing of key subjects. Furthermore, the exome sequencing did not detect any genetic variation at *PLTP* in addition to the known regulatory SNPs. However, as previously reported, these multiple regulatory region SNPs at *PLTP* did impact activity in these families (26). A chr. 2 linkage signal is supported but does not meet genome-wide significance (lod = 2.8), so we did not pursue it further.

Our study design presents several limitations. Nonexomic sites were not considered, so it is possible that a causal site is missed. Although it is possible that the variants in *LASS4* may be in LD with such a missed site, we believe coding variants are more likely to predict the large effect size detectable by linkage. Additionally, the exome coverage in the IBD region did not differ from other regions, indicating that it was likely that we detected all coding variation in this region in the exomed individuals. Second, several variants segregated with the IBD region, making it difficult to distinguish between those that may be causal and those that are in LD. To address this problem, we relied on effect in all families, as well as tissue expression and type of mutation to evaluate candidates in the IBD region. Additional QTLs in the genome may not have been detected because linkage analysis requires a large effect size as demonstrated by lack of linkage detection to the *PLTP* structural locus. Although the MCMC analyses can evaluate more complex models than some methods, the linear assumption may have hindered our efforts to detect a QTL that does not meet this requirement. Finally, the families were ascertained based on presence of FCHL. Although we lack evidence suggesting that PLTPa is associated with FCHL, it is possible that a relationship exists that could bias our analysis.

TABLE 5. The three *LASS4* haplotypes defined by SNPs rs17160348, rs36259, and rs17160349 in the CEU population

<i>LASS4</i> haplotype	HAPMAP frequency	aa 353	aa 366	aa 379
A	.80	ALA	ALA	ARG
B	.16	VAL	THR	GLN
C	.04	ALA	THR	ARG

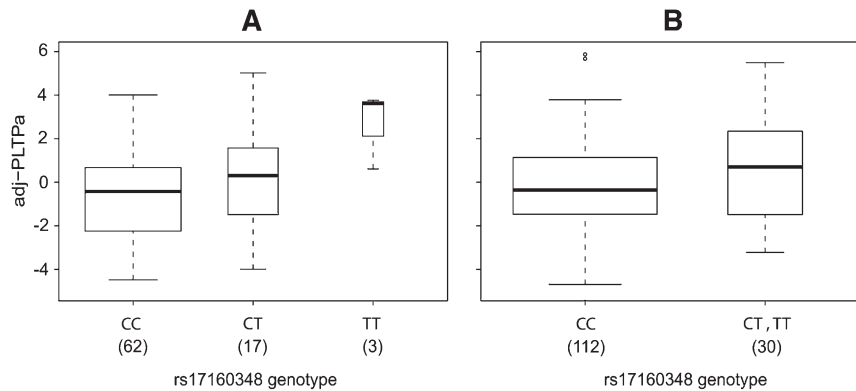


Fig. 4. Distribution of adj-PLTPa by *LASS4* rs17160348 genotype for (A) family F1 and (B) families F2, F3, and F4. The heterozygotes and minor homozygotes are combined in (B) because there are only two minor homozygotes, each from a different family. The width of each boxplot is proportional to the number of individuals with each genotype. Numbers in parentheses below the boxplots give the sample size. Refer to Fig. 1 for explanation of the boxplot symbols.

In summary, we detected evidence of linkage of PLTPa to chr. 19 in one family and chr. 2 in four families. This is the first evidence of genetic effects on PLTPa outside the *PLTP* structural locus. The availability of exome sequence data on selected individuals enabled analysis of one large region of the genome, presented here, and for future analysis on another large region on chr. 2. In addition, the availability of the exome sequence data enables analyses with these families on multiple traits without a priori knowledge of the regions of interest. In possibly the first example of using exome data in families to address a quantitative trait, our results suggest that variation in *LASS4* influences PLTPa in all four families. Furthermore, the *LASS4* variants accounted for slightly more variation in PLTPa than the *PLTP* SNP rs6065904, indicating that non-structural locus coding variation may be of interest when studying protein activity. Identification of genetic variation underlying PLTPa variation may illuminate the biology of PLTPa and ultimately impact the prevention and management of CVD. **■**

The authors thank the participating families, Laura McKinstry, Hiep Nguyen, Martha Horike-Pyne, Will Affleck-Asch, and Elizabeth Marchani.

REFERENCES

- Tall, A. R., S. Krumholz, T. Olivercrona, and R. J. Deckelbaum. 1985. Plasma phospholipid transfer protein enhances transfer and exchange of phospholipids between very low-density lipoproteins and high-density lipoproteins during lipolysis. *J. Lipid Res.* **26**: 842–851.
- Tu, A. Y., H. I. Nishida, and T. Nishida. 1993. High-density-lipoprotein conversion mediated by human plasma phospholipid transfer protein. *J. Biol. Chem.* **268**: 23098–23105.
- Jauhiainen, M., J. Metso, R. Pahlman, S. Blomqvist, A. Vantol, and C. Ehnholm. 1993. Human plasma phospholipid transfer protein causes high-density-lipoprotein conversion. *J. Biol. Chem.* **268**: 4032–4036.
- Wolfbauer, G., J. J. Albers, and J. F. Oram. 1999. Phospholipid transfer protein enhances removal of cellular cholesterol and phospholipids by high-density lipoprotein apolipoproteins. *Biochim. Biophys. Acta.* **1439**: 65–76.
- Tollefson, J. H., S. Ravnik, and J. J. Albers. 1988. Isolation and characterization of a phospholipid transfer protein (LTP-II) from human-plasma. *J. Lipid Res.* **29**: 1593–1602.
- Jiang, X. C., C. Bruce, J. Mar, M. Lin, Y. Ji, O. L. Francone, and A. R. Tall. 1999. Targeted mutation of plasma phospholipid transfer protein gene markedly reduces high-density lipoprotein levels. *J. Clin. Invest.* **103**: 907–914.
- Settasatian, N., M. N. Duong, L. K. Curtiss, C. Ehnholm, M. Jauhiainen, J. Huuskonen, and K. A. Rye. 2001. The mechanism of the remodeling of high density lipoproteins by phospholipid transfer protein. *J. Biol. Chem.* **276**: 26898–26905.
- Desrumaux, C. M., P. A. Mak, W. A. Boisvert, D. Masson, D. Stupack, M. Jauhiainen, C. Ehnholm, and L. K. Curtiss. 2003. Phospholipid transfer protein is present in human atherosclerotic lesions and is expressed by macrophages and foam cells. *J. Lipid Res.* **44**: 1453–1461.
- O'Brien, K. D., S. Vuletic, T. O. McDonald, G. Wolfbauer, K. Lewis, A. Y. Tu, S. Marcovina, T. N. Wight, A. Chait, and J. J. Albers. 2003. Cell-associated and extracellular phospholipid transfer protein in human coronary atherosclerosis. *Circulation.* **108**: 270–274.
- Jiang, X. C., O. L. Francone, C. Bruce, R. Milne, J. Mar, A. Walsh, J. L. Breslow, and A. R. Tall. 1996. Increased pre β -high density lipoprotein, apolipoprotein AI, and phospholipid in mice expressing the human phospholipid transfer protein and human apolipoprotein AI transgenes. *J. Clin. Invest.* **98**: 2373–2380.
- Jiang, X. C. 2002. The effect of phospholipid transfer protein on lipoprotein metabolism and atherosclerosis. *Front. Biosci.* **7**: d1634–d1641.
- Lie, J., R. de Crom, M. Jauhiainen, T. Van Gent, R. Van Haperen, L. Scheek, H. Jansen, C. Ehnholm, and A. Van Tol. 2001. Evaluation of phospholipid transfer protein and cholesteryl ester transfer protein as contributors to the generation of pre beta-high-density lipoproteins. *Biochem. J.* **360**: 379–385.
- van Haperen, R., A. van Tol, P. Venmeulen, M. Jauhiainen, T. van Gent, P. van den Beng, S. Ehnholm, F. Grosveld, A. van der Kamp, and R. de Crom. 2000. Human plasma phospholipid transfer protein increases the antiatherogenic potential of high density lipoproteins in transgenic mice. *Arterioscler. Thromb. Vasc. Biol.* **20**: 1082–1088.
- Lie, J., R. de Crom, T. van Gent, R. van Haperen, L. Scheek, F. Sadeghi-Niaraki, and A. van Tol. 2004. Elevation of plasma phospholipid transfer protein increases the risk of atherosclerosis despite lower apolipoprotein B-containing lipoproteins. *J. Lipid Res.* **45**: 805–811.
- Moerland, M., H. Samyn, T. van Gent, R. van Haperen, G. Dallinga-Thie, F. Grosveld, A. van Tol, and R. de Crom. 2008. Acute elevation of plasma PLTP activity strongly increases pre-existing atherosclerosis. *Arterioscler. Thromb. Vasc. Biol.* **28**: 1277–1282.
- Samyn, H., M. Moerland, T. van Gent, R. van Haperen, F. Grosveld, A. van Tol, and R. de Crom. 2009. Elevation of systemic PLTP, but not macrophage-PLTP, impairs macrophage reverse cholesterol transport in transgenic mice. *Atherosclerosis.* **204**: 429–434.

17. van Haperen, R., A. van Tol, T. van Gent, L. Scheek, P. Visser, A. van der Kemp, F. Grosveld, and R. de Crom. 2002. Increased risk of atherosclerosis by elevated plasma levels of phospholipid transfer protein. *J. Biol. Chem.* **277**: 48938–48943.
18. Yang, X. P., D. G. Yan, C. P. Qiao, R. J. Liu, J. G. Chen, J. Li, M. Schneider, L. Lagrost, X. Xiao, and X. C. Jiang. 2003. Increased atherosclerotic lesions in ApoE mice with plasma phospholipid transfer protein overexpression. *Arterioscler. Thromb. Vasc. Biol.* **23**: 1601–1607.
19. Jiang, X. C., S. C. Qin, C. P. Qiao, K. Kawano, M. Lin, A. Skold, X. Xiao, and A. R. Tall. 2001. Apolipoprotein B secretion and atherosclerosis are decreased in mice with phospholipid-transfer protein deficiency. *Nat. Med.* **7**: 847–852.
20. Luo, Y., L. Shelly, T. Sand, B. Reidich, G. Chang, M. MacDougall, M. Peakman, and X. Jiang. 2010. Pharmacologic inhibition of phospholipid transfer protein activity reduces apolipoprotein-B secretion from hepatocytes. *J. Pharmacol. Exp. Ther.* **332**: 1100–1106.
21. Albers, J. J., W. Pitman, G. Wolfbauer, M. Cheung, H. Kennedy, A. Tu, S. Marcovina, and B. Paigen. 1999. Relationship between phospholipid transfer protein activity and HDL level and size among inbred mouse strains. *J. Lipid Res.* **40**: 295–301.
22. Cheung, M. C., G. Wolfbauer, H. Deguchi, J. A. Fernandez, J. H. Griffin, and J. J. Albers. 2009. Human plasma phospholipid transfer protein specific activity is correlated with HDL size: implications for lipoprotein physiology. *Biochim. Biophys. Acta.* **1791**: 206–211.
23. Vergeer, M., S. M. Boekholdt, M. S. Sandhu, S. L. Ricketts, N. J. Wareham, M. J. Brown, U. de Faire, K. Leander, B. Gigante, M. Kavousi, et al. 2010. Genetic variation at the phospholipid transfer protein locus affects its activity and high-density lipoprotein size and is a novel marker of cardiovascular disease susceptibility. *Circulation.* **122**: 470–477.
24. Murdoch, S. J., M. C. Carr, J. E. Hokanson, J. D. Brunzell, and J. J. Albers. 2000. PLTP activity in premenopausal women: relationship with lipoprotein lipase, HDL, LDL, body fat, and insulin resistance. *J. Lipid Res.* **41**: 237–244.
25. Murdoch, S. J., M. C. Carr, H. Kennedy, J. D. Brunzell, and J. J. Albers. 2002. Selective and independent associations of phospholipid transfer protein and hepatic lipase with the LDL subfraction distribution. *J. Lipid Res.* **43**: 1256–1263.
26. Jarvik, G. P., R. Rajagopalan, E. A. Rosenthal, G. Wolfbauer, L. McKinsty, A. Vaze, J. Brunzell, A. G. Motulsky, D. A. Nickerson, P. J. Heagerty, et al. 2010. Genetic and non-genetic sources of variation in phospholipid transfer protein (PLTP) activity. *J. Lipid Res.* **51**: 983–990.
27. Riemens, S. C., A. van Tol, W. J. Sluiter, and R. P. F. Dullaart. 1999. Plasma phospholipid transfer protein activity is lowered by 24-h insulin and acipimox administration - blunted response to insulin in type 2 diabetic patients. *Diabetes.* **48**: 1631–1637.
28. Riemens, S. C., A. Van Tol, B. K. Stulp, and R. P. F. Dullaart. 1999. Influence of insulin sensitivity and the TaqIB cholesteryl ester transfer protein gene polymorphism on plasma lecithin:cholesterol acyltransferase and lipid transfer protein activities and their response to hyperinsulinemia in non-diabetic men. *J. Lipid Res.* **40**: 1467–1474.
29. Kathiresan, S., C. J. Willer, G. M. Peloso, S. Demissie, K. Musunuru, E. E. Schadt, L. Kaplan, D. Bennett, Y. Li, T. Tanaka, et al. 2009. Common variants at 30 loci contribute to polygenic dyslipidemia. *Nat. Genet.* **41**: 56–65.
30. Korstanje, R., J. J. Albers, G. Wolfbauer, R. H. Li, A. Y. Tu, G. A. Churchill, and B. J. Paigen. 2004. Quantitative trait locus mapping of genes that regulate phospholipid transfer activity in SM/J and NZB/BINJ Inbred Mice. *Arterioscler. Thromb. Vasc. Biol.* **24**: 155–160.
31. Badzioch, M. D., R. P. Igo, F. Gagnon, J. D. Brunzell, R. M. Krauss, A. G. Motulsky, E. M. Wijsman, and G. P. Jarvik. 2004. Low-density lipoprotein particle size loci in familial combined hyperlipidemia - evidence for multiple loci from a genome scan. *Arterioscler. Thromb. Vasc. Biol.* **24**: 1942–1950.
32. Wijsman, E. M., J. H. Rothstein, R. J. Igo, J. D. Brunzell, A. G. Motulsky, and G. P. Jarvik. 2010. Linkage and association analyses identify a candidate region for apoB level on chromosome 4q32.3 in FCHL families. *Hum. Genet.* **127**: 705–719.
33. Arnold, A. M., and R. A. Kronmal. 2003. Multiple imputation of baseline data in the cardiovascular health study. *Am. J. Epidemiol.* **157**: 74–84.
34. Durbin, J., and G. S. Watson. 1950. Testing for serial correlation in least squares regression. 1. *Biometrika.* **37**: 409–428.
35. Cheung, M. C., G. Wolfbauer, and J. J. Albers. 1996. Plasma phospholipid mass transfer rate: relationship to plasma phospholipid and cholesteryl ester transfer activities and lipid parameters. *Biochim. Biophys. Acta.* **1303**: 103–110.
36. Jarvik, G. P., L. S. Rozek, V. H. Brophy, T. S. Hatsukami, R. J. Richter, G. D. Schellenberg, and C. E. Furlong. 2000. Paraoxonase (PON1) phenotype is a better predictor of vascular disease than is PON1(192) or PON1(55) genotype. *Arterioscler. Thromb. Vasc. Biol.* **20**: 2441–2447.
37. Gagnon, F., G. P. Jarvik, M. D. Badzioch, A. G. Motulsky, J. D. Brunzell, and E. M. Wijsman. 2005. Genome scan for quantitative trait loci influencing HDL levels: evidence for multilocus inheritance in familial combined hyperlipidemia. *Hum. Genet.* **117**: 494–505.
38. Keating, B. J., S. Tischfield, S. S. Murray, T. Bhangale, T. S. Price, J. T. Glessner, L. Galver, J. C. Barrett, S. F. A. Grant, D. N. Farlow, et al. 2008. Concept, design and implementation of a cardiovascular gene-centric 50 K SNP array for large-scale genomic association studies. *PLoS ONE.* **3**: e3583.
39. Crawford, D. C., A. S. Nord, M. D. Badzioch, J. Ranchalis, L. A. McKinsty, M. Ahearn, C. Bertucci, C. Shephard, M. Wong, M. J. Rieder, et al. 2008. A common VLDLR polymorphism interacts with APOE genotype in the prediction of carotid artery disease risk. *J. Lipid Res.* **49**: 588–596.
40. Kong, X., K. Murphy, T. Raj, C. He, P. White, and T. Matise. 2004. A combined linkage-physical map of the human genome. *Am. J. Hum. Genet.* **75**: 1143–1148.
41. Haldane, J. B. S. 1919. The combination of linkage values, and the calculation of distances between the loci of linked factors. *J. Genet.* **8**: 299–309.
42. Ng, S. B., E. H. Turner, P. D. Robertson, S. D. Flygare, A. W. Bigham, C. Lee, T. Shaffer, M. Wong, A. Bhattacharjee, E. E. Eichler, et al. 2009. Targeted capture and massively parallel sequencing of 12 human exomes. *Nature.* **461**: 272–276.
43. McKenna, A., M. Hanna, E. Banks, A. Sivachenko, K. Cibulskis, A. Kernysky, K. Garimella, D. Altshuler, S. Gabriel, M. Daly, et al. 2010. The Genome Analysis Toolkit: A MapReduce framework for analyzing next-generation DNA sequencing data. *Genome Res.* **20**: 1297–1303.
44. Heath, S. C. 1997. Markov chain Monte Carlo segregation and linkage analysis for oligogenic models. *Am. J. Hum. Genet.* **61**: 748–760.
45. Igo, R. P. Jr, and E. M. Wijsman. 2008. Empirical significance values for linkage analysis: trait simulation using posterior model distributions from MCMC oligogenic segregation analysis. *Genet. Epidemiol.* **32**: 119–131.
46. Gagnon, F., G. Jarvik, A. Motulsky, S. Deeb, J. Brunzell, and E. Wijsman. 2003. Evidence of linkage of HDL level variation to APOC3 in two samples with different ascertainment. *Hum. Genet.* **113**: 522–533.
47. Igo, R., N. Chapman, V. Berninger, M. Matsushita, Z. Brkanac, J. Rothstein, T. Holzman, K. Nielsen, W. Raskind, and E. Wijsman. 2006. Genomewide scan for real-word reading subphenotypes of dyslexia: novel chromosome 13 locus and genetic complexity. *Am. J. Med. Genet. B Neuropsych. Genet.* **141B**: 15–27.
48. Rosenthal, E. A., and E. M. Wijsman. 2010. Joint linkage and segregation analysis under multiallelic trait inheritance: simplifying interpretations for complex traits. *Genet. Epidemiol.* **34**: 344–353.
49. Thompson, E. A. 2005. MCMC in the analysis of genetic data on pedigrees. In *Markov Chain Monte Carlo: Innovations and Applications*. F. Liang, J. Wang, and W. Kendall, editors. World Scientific Co. Pte. Ltd., Singapore. 183–216.
50. Wijsman, E. M., J. H. Rothstein, and E. A. Thompson. 2006. Multipoint linkage analysis with many multiallelic or dense diallelic markers: Markov chain-Monte Carlo provides practical approaches for genome scans on general pedigrees. *Am. J. Hum. Genet.* **79**: 846–858.
51. Tong, L., and E. A. Thompson. 2008. Multilocus lod scores in large pedigrees: combination of exact and approximate calculations. *Hum. Hered.* **65**: 142–153.
52. Kleensang, A., D. Franke, A. Alcais, L. Abel, B. Mueller-Myhsok, and A. Ziegler. 2010. An extensive comparison of quantitative trait loci mapping methods. *Hum. Hered.* **69**: 202–211.
53. Clerget-Darpoux, F., M. C. Babron, B. Prum, G. M. Lathrop, I. Deschamps, and J. Hors. 1988. A new method to test genetic models in HLA associated diseases: the MASC method. *Ann. Hum. Genet.* **52**: 247–258.
54. Amos, C. I., and M. de Andrade. 2001. Genetic linkage methods for quantitative traits. *Stat. Methods Med. Res.* **10**: 3–25.

55. Clerget-Darpoux, F., C. Bonaiti-Pellie, and J. Hochez. 1986. Effects of misspecifying genetic parameters in lod score analysis. *Biometrics*. **42**: 393–399.
56. Greenberg, D. A., P. Abreu, and S. E. Hodge. 1998. The power to detect linkage in complex disease by means of simple LOD-score analyses. *Am. J. Hum. Genet.* **63**: 870–879.
57. Ott, J. 1999. *Analysis of Human Genetic Linkage*. The Johns Hopkins University Press, Baltimore.
58. Thompson, E. 2011. The structure of genetic linkage data: from LIPED to 1M SNPs. *Hum. Hered.* **71**: 86–96.
59. Boerwinkle, E., R. Chakraborty, and C. F. Sing. 1986. The use of measured genotype information in the analysis of quantitative phenotypes in Man. I. models and analytical methods. *Ann. Hum. Genet.* **50**: 181–194.
60. Almasy, L., and J. Blangero. 2004. Exploring positional candidate genes: linkage conditional on measured genotype. *Behav. Genet.* **34**: 173–177.
61. Göring, H. H. H., J. D. Terwilliger, and J. Blangero. 2001. Large upward bias in estimation of locus-specific effects from genomewide scans. *Am. J. Hum. Genet.* **69**: 1357–1369.
62. Almasy, L., and J. Blangero. 1998. Multipoint quantitative-trait linkage analysis in general pedigrees. *Am. J. Hum. Genet.* **62**: 1198–1211.
63. Dixon, W. J., and J. W. Tukey. 1968. Approximate behavior of distribution of Winsorized T (Trimming/winsorization 2). *Technometrics*. **10**: 83–98.
64. Rivest, L. P. 1994. Statistical properties of Winsorized means for skewed distributions. *Biometrika*. **81**: 373–383.
65. Adzhubei, I. A., S. Schmidt, L. Peshkin, V. E. Ramensky, A. Gerasimova, P. Bork, A. S. Kondrashov, and S. R. Sunyaev. 2010. A method and server for predicting damaging missense mutations. *Nat. Methods*. **7**: 248–249.
66. Altshuler, D. L. and 1000 Genomes Project Consortium. 2010. A map of human genome variation from population-scale sequencing. *Nature*. **467**: 1061–1073.
67. Mukhopadhyay, A., S. Talukdar, A. Bhattacharjee, and K. Ray. 2004. Bioinformatic approaches for identification and characterization of olfactomedin related genes with a potential role in pathogenesis of ocular disorder. *Mol. Vis.* **10**: 304–314.
68. Schadt, E. E., C. Molony, E. Chudin, K. Hao, X. Yang, P. Y. Lum, A. Kasarskis, B. Zhang, S. Wang, C. Suver, et al. 2008. Mapping the genetic architecture of gene expression in human liver. *PLoS Biol.* **6**: e107.
69. Mizutani, Y., A. Kihara, and Y. Igarashi. 2005. Mammalian Lass6 and its related family members regulate synthesis of specific ceramides. *Biochem. J.* **390**: 263–271.
70. Wu, D., Z. Ren, M. Pae, W. Guo, X. Cui, A. H. Merrill, and S. N. Meydani. 2007. Aging up-regulates expression of inflammatory mediators in mouse adipose tissue. *J. Immunol.* **179**: 4829–4839.
71. Schuler, G. D. 1997. Pieces of the puzzle: expressed sequence tags and the catalog of human genes. *J. Mol. Med.* **75**: 694–698.
72. Pontius, J. U., L. Wagner, and G. D. Schuler. 2003. UniGene: a unified view of the transcriptome. In *The NCBI Handbook*. J. McEntyre and J. Ostell, editors. National Center for Biotechnology Information, Bethesda, MD. Chapter 21. 1–11.
73. Hicks, A. A., P. P. Pramstaller, A. Johansson, V. Vitart, I. Rudan, P. Ugozai, Y. Aulchenko, C. S. Franklin, G. Liebisch, J. Erdmann, et al. 2009. Genetic determinants of circulating sphingolipid concentrations in European populations. *PLoS Genet.* **5**: e1000672.
74. Bonzón-Kulichenko, E., D. Schwudke, N. Gallardo, E. Molto, T. Fernandez Agullo, A. Shevchenko, and A. Andres. 2009. Central leptin regulates total ceramide content and sterol regulatory element binding protein-1C proteolytic maturation in rat white adipose tissue. *Endocrinology*. **150**: 169–178.